Applied Surface Science 258 (2012) 3829–3834

Contents lists available at SciVerse ScienceDirect

Applied Surface Science

journal homepage: www.elsevier.com/locate/apsusc

Optical properties and chemical structures of Kapton-H film after proton irradiation by immersion in a hydrogen plasma

Jingwei Shi[a], Chunzhi Gong[a], Xiubo Tian[a,*], Shiqin Yang[a], Paul K. Chu[b]

[a] State Key Laboratory of Advanced Welding and Joining, Harbin Institute of Technology, Harbin 150001, China
[b] Department of Physics & Materials Science, City University of Hong Kong, Tat Chee Avenue, Kowloon, Hong Kong

A R T I C L E I N F O

Article history:
Received 18 October 2011
Received in revised form 8 December 2011
Accepted 8 December 2011
Available online 29 December 2011

Keywords:
Proton irradiation
Kapton-H
Hydrogen plasma immersion configuration
Optical transmittance
Bonds breakage

A B S T R A C T

Proton irradiation of Kapton-H films was physically simulated in plasma immersion configuration with hydrogen plasmas. Hydrogen ion was implanted into the samples biased to a negative pulse of 20 kV. Optical transmittance of the sample in the wavelength region of 200–2500 nm was determined by a UV–vis–NIR scanning spectrophotometer, and the functional group evolution was examined by X-ray photoelectron spectroscopy (XPS). Atomic force microscopy (AFM) was utilized to determine the roughness and morphology of the samples, and the bulk modification was analyzed by FTIR. The experimental results showed the optical transmittance of the treated sample in the wavelength of 500–2000 nm weakened after proton irradiation, and decreased with the increase of irradiation time. Finger-like bulges emerged on the surface of the sample irradiated by ion irradiation for 30 min, and became bigger and denser with the increase of the irradiation time. The content of C element of the sample increased after proton irradiation, while that of N and O elements decreased because of the bonds breakage of C=O, C—O—C and C—N during irradiation process.

1. Introduction

Polyimide (PI) is widely applied in spacecrafts like artificial satellites and space stations as thermal blanket and insulating materials due to its light weight, outstanding physical properties, excellent thermal stability, attractive dielectric properties and high resistance to space environment irradiation [1–3]. Space protons, one important part of the space environment factors [4,5], could significantly degrade the surface properties of polyimide films due to their high kinetic energy and wide abundance in space [6]. Experimental results have demonstrated that failure stress and strain of polyimide films decreased significantly as a result of proton irradiation [4], while the surface hardness increased with the increase of the incident flounce [7]. Chemical bonds breakage of polyimide films irradiated by protons has also been testified [8,9]. The radiation-induced scission of chemical bonds dominated the performance degradation of polyimide films irradiated by protons [10] and reflection spectra and hemispherical emittance of polyimide films after proton irradiation also changed which led to an increase of solar absorptance and temperature change [3,11].

The ion irradiation effect on polyimide films has been investigated by ground-based simulation experiment using ion beam irradiation technique [12,13]. Plasma immersion ion implantation (PIII) [14,15] has proven to be an effective and costless surface processing tool, which can be utilized to realize ion implantation into both metal substrates and insulating samples [16,17]. Proton irradiation of polyimide films can be conducted when hydrogen plasma is utilized in the PIII process. This may lead to the advantages of low cost, high efficiency over traditional proton irradiation systems [4]. Moreover, large size specimen can be simultaneously processed and multiple ion energies may be achieved, which is more alike those in the practical space environment. In the present work, commercially available polyimide films (Kapton-H) are irradiated in hydrogen plasma immersion configuration, and spectral transmittance, surface morphology and chemical structure of Kapton-H films before and after proton irradiation are investigated.

2. Experiment details

Kapton-H samples (50.8 μm thick, DuPont) were ultrasonically cleaned in anhydrous ethyl alcohol for 20 min and dried using cool air before loaded into the vacuum chamber, and then proton irradiation process was performed in a plasma immersion ion implanter as shown in Fig. 1. The experimental set-up comprised a vacuum chamber and pumping system, a substrate holder, a hydrogen provider, a plasma source and a pulsed high-voltage power supply. The vacuum chamber was pumped to a base pressure of 1×10^{-2} Pa and the operating pressure (0.5 Pa) was achieved by

---

* Corresponding author. Tel.: +86 451 86418784; fax: +86 451 86418784.
E-mail address: xiubotian@163.com (X. Tian).

0169-4332/$ – see front matter © 2011 Elsevier B.V. All rights reserved.
doi:10.1016/j.apsusc.2011.12.037

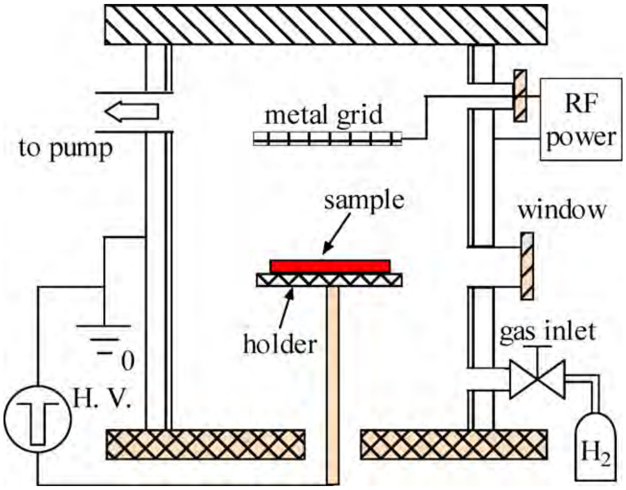

Fig. 1. Schematic diagram of the experimental set-up.

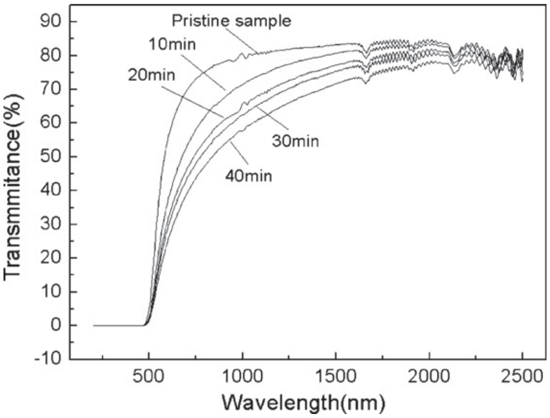

Fig. 2. Spectral transmittance of the pristine sample and samples irradiated for 10 min, 20 min, 30 min and 40 min, respectively.

introducing H_2 (20 sccm) through a mass flowmeter. Capacitively coupled radio-frequency (13.56 MHz) discharge was employed to generate hydrogen plasmas for proton irradiation. The Kapton-H film was located on the sample holder. High voltage pulses with the amplitude of 20 kV, repetition rate of 200 Hz and pulse duration of 20 μs were applied to the metal holder. RF power was kept at 200 W and the irradiation time was 10 min, 20 min, 30 min and 40 min, respectively. Optical properties of the samples were measured by using a UV–vis–NIR scanning spectrophotometer immediately after the samples were taken out of the chamber. The surface morphology and average roughness of Kapton-H samples before and after irradiation were investigated by using atomic force microscopy (AFM) in the contact mode. Elemental composition of the surface layer was determined by X-ray photoelectron spectroscopy (XPS) and the C 1s, N 1s and O 1s spectra were decomposed by fitting a Gaussian–Lorentzian mixture function (Gaussian: 80%, Lorentzian: 20%) on a Shirley background [18]. Bulk modifications in the samples were evaluated by Fourier transformed infrared spectroscopy (FTIR) which recorded the transmittance spectra of the samples before and after proton irradiation in the range from 2400 cm^{-1} to 800 cm^{-1}.

3. Results and discussion

Fig. 2 shows the spectral transmittance spectra of the Kapton-H films before proton irradiation and irradiated for different time. For pristine sample, the transmittance is almost zero in the wavelength region of 200–500 nm and 80% in the range of 1000–2500 nm [11]. It is attributed to the presence of the chromophores such as C=O and aromatic ring which have a strong complicated absorption in the ultraviolet region [19]. After proton irradiation, a strong decrease of spectral transmittance is observed in the visible and infrared region. It is due to the formation of new chromophores and auxochromes [9], and spectral transmittance also decreases with the increase of the irradiation time as reported in the literatures [20].

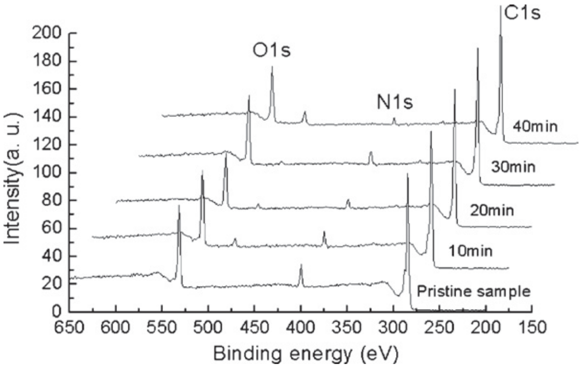

Fig. 3. XPS survey spectrum of the pristine sample and samples irradiated for 10 min, 20 min, 30 min and 40 min, respectively.

Fig. 3 displays XPS survey spectra of Kapton-H films before and after proton irradiation. The peaks of the binding energy of 285 eV, 532 eV and 400 eV correspond to C 1s, O 1s and N 1s, respectively [2,21], and the intensity of these peaks changes substantially after proton irradiation as in Ref. [8]. Fig. 4 demonstrates the concentration of carbon, oxygen and nitrogen on the top surface of the samples. It is evident that the elemental concentration of both nitrogen and oxygen reduces. The elemental content of carbon increases with the increase of irradiation time, resulting in carbonization.

For the pristine sample, the C:O and C:N ratios are found to be 4.2 and 12.2, respectively, while they are 4.6 and 23.4 for the sample irradiated by protons for 40 min, respectively. The increase of C:O and C:N ratios indicates that a significant loss of oxygen and nitrogen on the surface of the sample after proton irradiation happens due to the bond breakage of C=O, C—O and C—N [22,23].

Fig. 5 and Fig. 6 present the curve-fitted high-resolution XPS spectra obtained from the pristine sample and sample irradiated by protons for 40 min, respectively. For the pristine sample, four different carbon environments in the C 1s region are utilized as shown in Fig. 5(a) [19,21,24]: (1) carbon atom bonded from the aromatic rings that are not directly attached to the imide ring at 284.7 eV (C—C); (2) carbon atoms bonded to nitrogen (C—N) and carbon atom bonded from the aromatic rings in the imide group at 285.6 eV; (3) carbon atoms bonded to oxygen related to the ether group (C—O) at 286.3 eV and (4) carbon atoms bonded to oxygen in the imide ring at 288.6 eV assigned to the carbonyl group (C=O). In the O 1s region, two components are detected at 531.9 eV and 533.1 eV, arising from the carbonyl group (C=O) in the imide systems and the ether group (C—O), respectively. Only one symmetric peak at 400.4 eV (C—N) was found for the N 1s region. For the Kapton-H sample irradiated by protons for 40 min, changes in the peak shape and position of C 1s, O 1s and N 1s spectra are observed, indicating that the chemical environment has been altered, and no new peaks are available in the spectra.

Curve-fitted peak position and the area of C 1s, O 1s and N 1s for the pristine sample and sample irradiated for 40 min are summarized in Table 1. For the C 1s region, the decrease of peak areas at 288.6 eV (C=O) and 286.3 eV (C—O) indicates that C=O and C—O bonds have been broken and oxygen atoms are released, while the peak area at 284.7 eV (C—C) increases, which could be related to

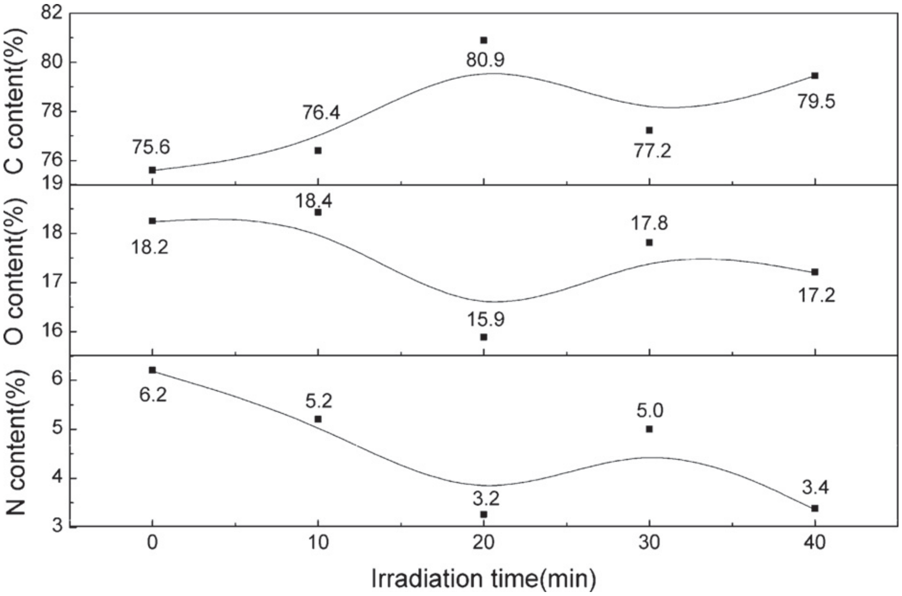

Fig. 4. Surface composition of Kapton-H films before and after proton irradiation as measured by XPS.

a new covalent bonded structure mainly constructed by phenyl [8]. In the O 1s spectrum, the peak area corresponding to 531.9 eV (C=O) decreases, while the peak area at 533.1 eV (C—O) increases correspondingly, indicating that more carbonyl (C=O) bonds than aromatic ether (C—O) bonds are broken during proton irradiation process. Moreover, the symmetry of the N 1s spectrum is not broken after proton irradiation as shown in Fig. 6(c).

Fig. 7 depicts FTIR transmission spectra of Kapton-H films before and after proton irradiation. The spectrum configuration is similar no matter whether the sample is irradiated or not. It indicates no major bulk modification of the Kapton-H films after proton irradiation [23]. However, there is an overall reduction in the intensities of all the characteristic peaks for the irradiated samples. The peaks at 1775 cm^{-1} and 1718 cm^{-1} correspond to asymmetric C=O

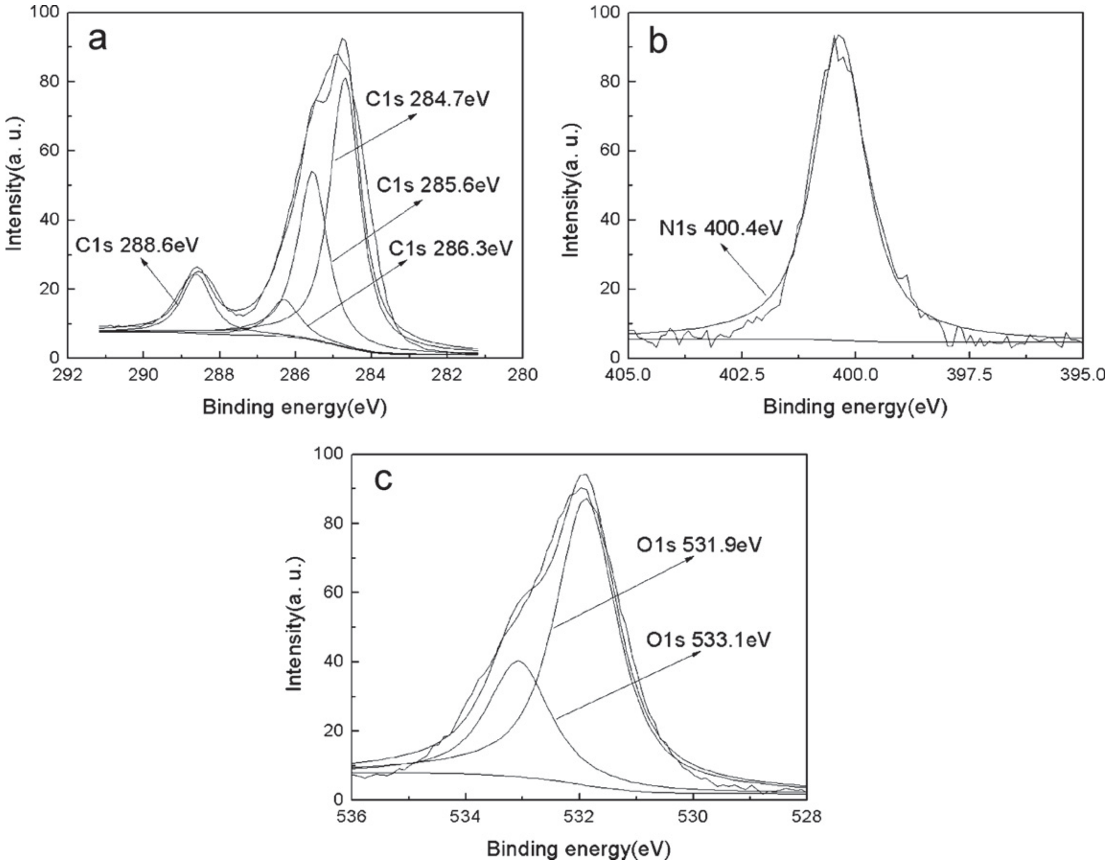

Fig. 5. Peak fitting XPS spectra of (a) C 1s, (b) N 1s and (c) O 1s of the pristine sample.

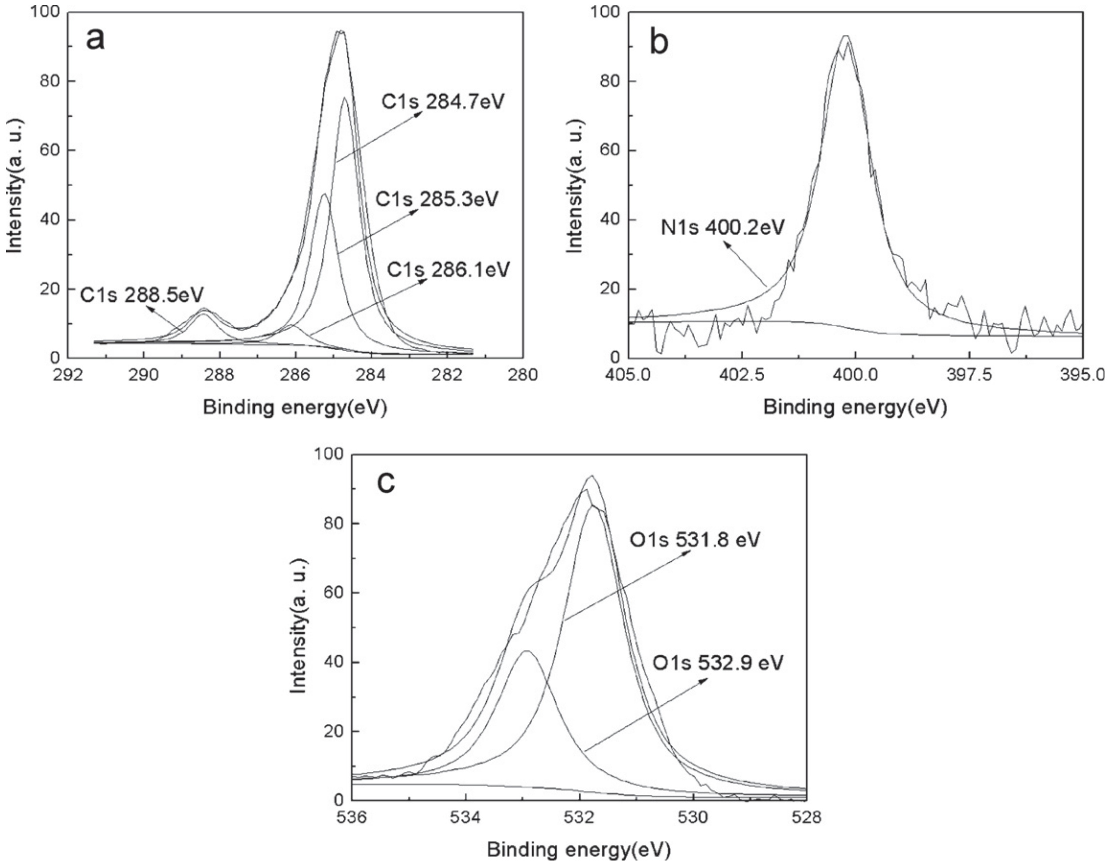

Fig. 6. Peak fitting XPS spectra of (a) C 1s, (b) N 1s, and (c) O 1s of the sample irradiated by protons for 40 min.

Table 1
Results of the peak separation of XPS spectra, together with the binding energy and the peak areas of the spectra.

Peak	Pristine sample		Sample irradiated for 40 min	
	E_b (eV)	Area (%)	E_b (eV)	Area (%)
C	284.7	50.52	284.7	55.32
1s	285.6	31.61	285.3	33.72
	286.3	6.89	286.1	4.40
	288.6	10.98	288.4	6.55
N 1s	400.4	100%	400.2	100%
O	531.9	71.59	531.8	67.80
1s	533.1	28.41	532.9	32.20

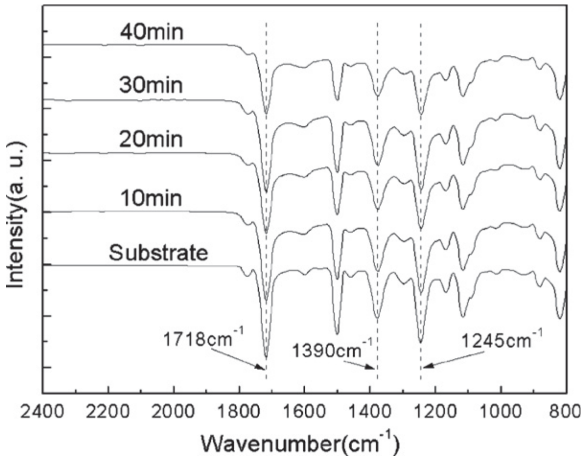

Fig. 7. FTIR spectra of the pristine sample and samples irradiated for 10 min, 20 min, 30 min and 40 min, respectively.

Table 2
Roughness for the pristine sample and samples irradiated by protons for various time.

Irradiation time (min)	0	10	20	30	40
R_a (nm)	0.835	0.534	0.978	0.299	1.406
R_{max} (nm)	22.026	8.689	16.661	10.184	54.310

stretching vibration and symmetric C═O stretching vibration, respectively. Aromatic C—C stretching vibration is presented at 1501 cm^{-1} and C—N stretching vibration is presented at 1390 cm^{-1}. The peak at 1245 cm^{-1} designated to Asymmetric C—O—C stretching can be readily observed, and the peak at 820 cm^{-1} is ascribed to multi substituted aromatic C—C stretching vibration [25,26]. Changes in the spectra of the irradiated samples indicate that some complex chemical reactions occur during proton irradiation process, including the bond breakage of the carbonyl (C═O) and aromatic ether (C—O—C) and ring opening reaction of cyclic imide (C—N) [9], which are consist with what XPS results describe.

Surface morphology of the pristine sample and samples irradiated by protons for various time is examined by AFM. The images of the 5 μm × 5 μm surface area of the samples are shown in Fig. 8(a)–(e). The original surface of the sample is flat and smooth before irradiation, and some small finger-like bulges appear on the surface of the sample irradiated for 30 min as shown in Fig. 8(d). The density and the size of the finger-like bulges increases with the irradiation time, which can be attributed to the surface etching and the polymer chains breakage by energetic protons in a selective manner [8,27]. An arithmetic mean of the surface roughness (R_a) and the maximum height (R_{max}) listed in Table 2 are calculated from the roughness profile determined by AFM. A small decrease in surface roughness of Kapton-H samples is observed after irradiated for

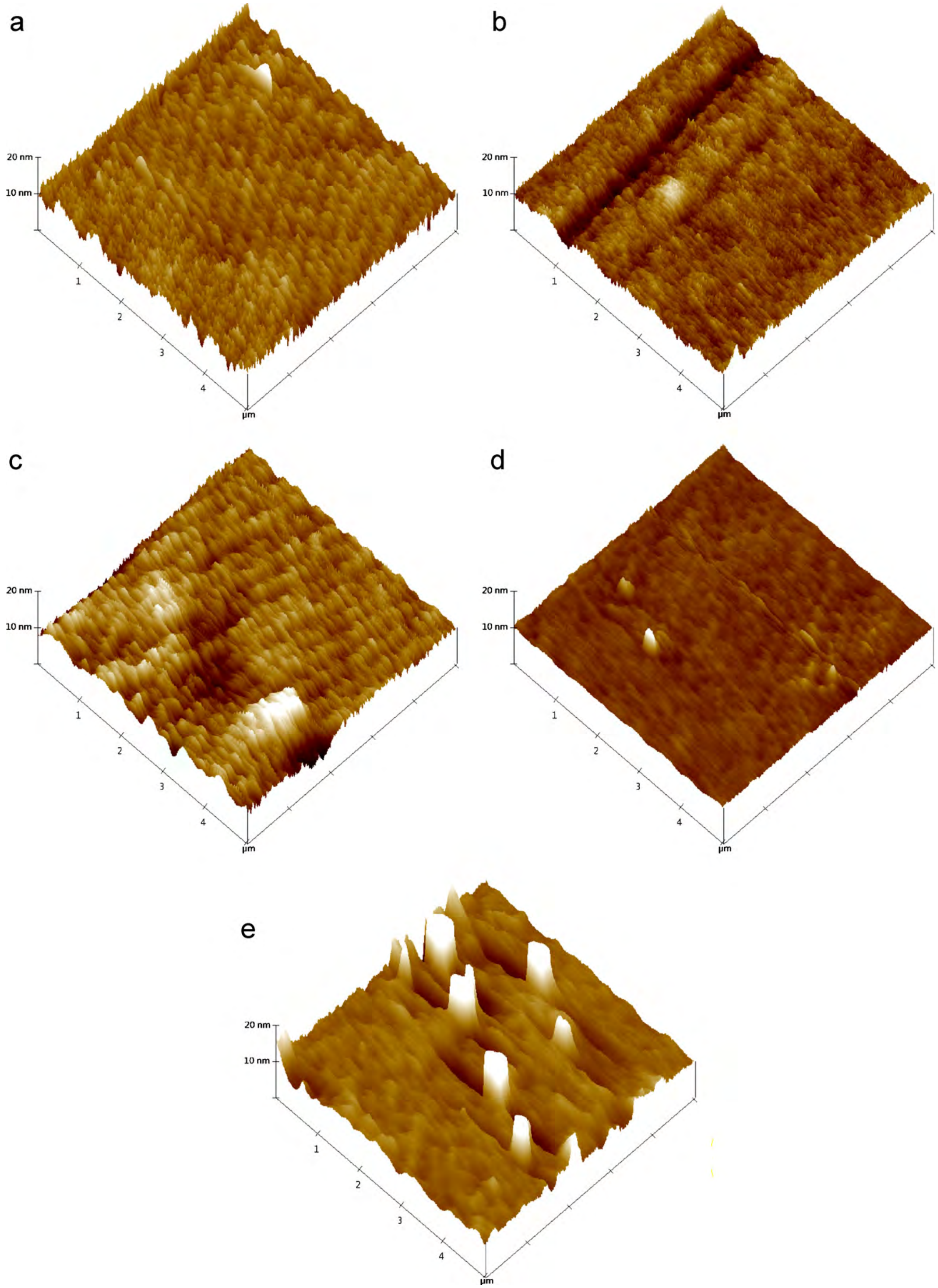

Fig. 8. AFM image of Kapton-H films (a) before irradiation, and irradiated by protons for (b) 10 min, (c) 20 min, (d) 30 min and (e) 40 min, respectively.

less than 30 min. In contrast, for the 40 min treated sample, a sharp increase in surface roughness is observed due to the emergence of abundant finger-like bulges.

During the proton irradiation process, UV radiation on and thermal effect of samples may occur. The spectral transmittance of Kapton films decreases in the visible and near infrared zones, and the absorption line red-shifts is observed after UV radiation [28]. However, the transmittance spectra of the samples shows no red-shifts (Fig. 2) meaning that the effect of UV radiation on Kapton-H films is slight. It has been reported that the thermal emittance of the samples hardly changes under simultaneous UV, electron, and proton radiation [4], inferring that Kapton films have the high-thermal stability [3]. In fact, during the experiments the 200 W RF power is coupled to the antenna, not directly applied to the samples, and thus thermal effect of Kapton films may not be significant. The loss of volatile groups such as $\mathrm{C{-}O}$ and $\mathrm{C{-}N}$ may arise as a result of UV radiation as shown in Fig. 6 and tensile strength degradation may be induced [4,23].

4. Conclusion

Proton irradiation on Kapton-H films is realized using hydrogen plasma immersion configuration. This makes it possible to irradiate large area samples with a costless mode and a little higher similarity to practical space environments. The decrease in spectral transmittance of the samples irradiated by protons is observed in the wavelength of 500–2500 nm, and the spectral transmittance decreases with the increase of the irradiation time. The surface concentration of C element increases while that of N element and O element decreases. This is attributed to the bond breakage of $\mathrm{C{-}N}$, $\mathrm{C{=}O}$ and $\mathrm{C{-}O{-}C}$. The transmission spectrum of the samples after proton irradiation degrades in all the characteristic peaks. The finger-like bulges emerge on the surface of Kapton-H films after irradiation, which depends on processing time.

Acknowledgment

This research was supported by the Natural Science Foundation of China under grant no. 50773015.

References

[1] V.E. Skurat, E.A. Barbashev, Y.I. Dorofeev, A.P. Nikiforov, M.M. Gorelova, A.I. Pertsyn, Appl. Surf. Sci. 92 (1996) 441.

[2] R.L. Kiefer, W.J. Gabler, M.T. Hovey, S.A. Thibeaul, Radiat. Phys. Chem. 80 (2011) 126.

[3] M. Iwata, A. Ohnishi, H. Hirosawa, F. Tohyama, J. Spacecraft Rockets 38 (2001) 504.

[4] D.A. Russell, J.W. Connell, L.B. Fogdall, J. Spacecraft Rockets 39 (2002) 833.

[5] A.N. Petrov, O.R. Grigoryan, N.V. Kuznetsov, Adv. Space Res. 43 (2009) 654.

[6] H.B. Garrett, D. Hastings, AIAA 0590 (1994) 1.

[7] N. Shah, N.L. Singh, C.F. Desai, K.P. Singh, Radiat. Meas. 36 (2003) 699.

[8] R.Q. Li, C.D. Li, S.Y. He, M.W. Di, D.Z. Yang, Radiat. Phys. Chem. 77 (2008) 482.

[9] R.Q. Li, C.D. Li, S.Y. He, M.W. Di, D.Z. Yang, Radiat. Phys. Chem. 76 (2007) 1200.

[10] R. Artiaga, M. Chipara, C.P. Stephens, R.S. Benson, Nucl. Instrum. Methods B 236 (2005) 432.

[11] M.M. Mikhailov, C.D. Li, D.C. Jan, Russ. Phys. J. 43 (2000) 552.

[12] S. Pylypenko, K. Artyushkova, J.E. Fulghum, Appl. Surf. Sci. 256 (2010) 3204.

[13] J.P. Jeun, J.W. Shin, Y.C. Nho, P.H. Kang, J. Ind. Eng. Chem. 15 (2009) 56.

[14] J.R. Conrad, J.L. Radtke, R.A. Dodd, F.J. Worzala, J. Appl. Phys. 62 (1987) 4591.

[15] J.R. Conrad, R.A. Dodd, F.J. Worzala, X. Qiu, Surf. Coat. Technol. 36 (1988) 927.

[16] W. Zhang, P.K. Chu, J.H. Ji, Y.H. Zhang, X.Y. Liu, R.K.Y. Fu, P.C.T. Ha, Q. Yan, Biomaterials 27 (2006) 44.

[17] X.B. Tian, S.Q. Yang, Y.X. Huang, P.K. Chu, R.K.Y. Fu, J. Phys. D 37 (2004) 50.

[18] M.G. Han, S.S. Im, Polymer 41 (2000) 3253.

[19] Y.X. Huang, X.B. Tian, S.Q. Yang, R.K.Y. Fu, P.K. Chu, Appl. Surf. Sci. 253 (2007) 9483.

[20] G. Compagnini, G. Foti, R. Reitano, G. Mondio, Appl. Phys. Lett. 57 (1990) 2546.

[21] A.M. Ektessabi, S. Hakamata, Thin Solid Films 377 (2000) 621.

[22] X.L. Xu, D. Xu, Z.X. Lin, G.D. Du, Z.Y. Zhou, S.Q. Yang, L.Z. Chen, G.Q. Xia, S.C. Zou, Prog. Nat. Sci. 2 (1992) 438.

[23] K.P. Adhia, R.L. Owings, T.A. Railkar, W.D. Brown, A.P. Malshe, Appl. Surf. Sci. 225 (2004) 324.

[24] G. Beamson, D. Briggs, The Scienta ESCA300 Database, John Wiley & Sons, 1992.

[25] Z.F. Wu, Y.C. Shi, H.M. Chen, C.Y. Fang, Chin. Sci. Bull. 38 (1993) 510.

[26] B.P. Singh, D. Singh, R.B. Mathur, T.L. Dhami, Nanoscale Res. Lett. 3 (2008) 444.

[27] T. Shao, C. Zhang, K.H. Long, D.D. Zhang, J. Wang, P. Yan, Y.X. Zhou, Appl. Surf. Sci. 256 (2010) 3888.

[28] G.R. Peng, W.G. Hao, D.Z. Yang, S.Y. He, J. Appl. Polym. Sci. 94 (2004) 1370.